$K^+ \to \pi^+\pi^0\gamma$ in the Standard Model and Beyond

P. MERTENS
Centre for Cosmology, Particle Physics and Phenomenology (CP3)
Université catholique de Louvain, Chemin du Cyclotron, 2
B-1348 Louvain-la-Neuve, Belgium

In this note we show how improved theoretical analysis combined with recent experimental data coming from NA48/2 concerning $K^+ \to \pi^+\pi^0\gamma$ decay shed light on the dynamics of the $s \to d\gamma$ transition. Consequences on NP analysis are also presented.

1 Introduction

In the search for New Physics (NP) the $s \to d\gamma$ process is complementary to $b \to s\gamma$ and $\mu \to e\gamma$, as the relative strength of these transitions is a powerful tool to investigate the NP dynamics. However, since $s \to d\gamma$ takes place deep within the non-perturbative regime of QCD we have to control hadronic effects and find observables sensitive to the short-distance dynamics, and thereby to possible NP contributions. The purpose of this note is to show how this can be achieved using the $K^+ \to \pi^+\pi^0\gamma$ observable [1].

In section 2, the anatomy of the $s \to d\gamma$ process in the Standard Model (SM) is shortly detailed. In section 3, we analyse the $K^+ \to \pi^+\pi^0\gamma$ decay in the SM whereas section 4 is devoted to show how, in the MSSM, rare and $K^+ \to \pi^+\pi^0\gamma$ decays, as well as $\mathrm{Re}(\varepsilon'_K/\varepsilon_K)$ can be exploited to constrain NP.

2 The $s \to d\gamma$ anatomy

In the SM, the flavour changing electromagnetic process $s \to d\gamma$ is a loop effects which at low energy scale is described by the effective $\Delta S = 1$ Hamiltonian [2]

$$\mathcal{H}_{eff}(\mu \approx 1\ \text{GeV}) = \sum_{i=1}^{10} C_i\,(\mu)\,Q_i\,(\mu) + C^{\pm}_{\gamma^*}Q^{\pm}_{\gamma^*} + C^{\pm}_{\gamma}Q^{\pm}_{\gamma} + h.c.\ , \tag{1}$$

where the Q_i are effective four-quarks operators whereas the quark-bilinear electric $Q^{\pm}_{\gamma^*}$ and magnetic $Q^{\pm}_{\gamma}$ operators are respectively given by[a] $Q^{\pm}_{\gamma^*} = (\bar{s}_L\gamma^\nu d_L \pm \bar{s}_R\gamma^\nu d_R)\,\partial^\mu F_{\mu\nu}$ and $Q^{\pm}_{\gamma} = (\bar{s}_L\sigma^{\mu\nu}d_R \pm \bar{s}_R\sigma^{\mu\nu}d_L)\,F_{\mu\nu}$. In the non perturbative regime of QCD this Hamiltonian is hadronized into an effective weak Lagrangian that shares the chiral properties of the operators contained in $\mathcal{H}_{eff}$. The chiral structures of Q_i and $Q^{\pm}_{\gamma^*}$ allow the usual $\mathcal{O}(p^2)$ weak Lagrangian $\mathcal{L}_W = G_8O_8 + G_{27}O_{27} + G_{ew}O_{ew}$ (detailed in [10]) whereas the chirality flipping $Q^{\pm}_{\gamma}$ operators induce more involved $\mathcal{O}(p^4)$ local interactions (detailed in [1,10]). The non-trivial dynamics corresponding to

[a] By definition : $2\sigma^{\mu\nu} = i[\gamma^\mu, \gamma^\nu]$.

the low-energy tails of the photon penguins arise at $\mathcal{O}(p^4)$ (the $\mathcal{O}(p^2)$ dynamics being completely predicted by Low's theorem [3]) where they are represented in terms of non-local meson loops, as well as additional $\mathcal{O}(p^4)$ local effective interactions, in particular the $\Delta I = 1/2$ enhanced $N_{14}, ..., N_{18}$ octet counterterms [4, 5].

3 $K^+ \to \pi^+\pi^0\gamma$ in the SM

For the $K^+ \to \pi^+\pi^0\gamma$ decay, the standard phase-space variables are chosen as the π^+ kinetic energy T_c^* and $W^2 \equiv (q_\gamma \cdot P_K)(q_\gamma \cdot P_{\pi^+})/m_{\pi^+}^2 m_K^2$ [6]. Indeed, pulling out the dominant bremsstrahlung contribution, the differential rate can be written

$$\frac{\partial^2\Gamma}{\partial T_c^* \partial W^2} = \frac{\partial^2\Gamma_{IB}}{\partial T_c^* \partial W^2}\left(1 - 2\frac{m_{\pi^+}^2}{m_K}\operatorname{Re}\left(\frac{E_{DE}}{eA_{IB}}\right)W^2 + \frac{m_{\pi^+}^4}{m_K^2}\left(\left|\frac{E_{DE}}{eA_{IB}}\right|^2 + \left|\frac{M_{DE}}{eA_{IB}}\right|^2\right)W^4\right) . \quad (2)$$

In this expression both electric E_{DE} and magnetic M_{DE} direct emission amplitudes are functions of W^2 and T_c^* and appear at $\mathcal{O}(p^4)$. To a very good approximation we can identify these direct emission amplitudes with their first multipole for which the $\pi^+\pi^0$ state is in a P wave. The main interest of $K^+ \to \pi^+\pi^0\gamma$ is that its bremsstrahlung component $A_{IB} = A(K^+ \to \pi^+\pi^0)$ is pure $\Delta I = 3/2$ hence suppressed, making the direct emission amplitudes easier to access. The magnetic amplitude M_{DE} is dominated by the QED anomaly and will not concern us here.

3.1 Differential rate

Given its smallness, we can assume the absence of CP-violation when discussing this observable. Experimentally, the electric and magnetic amplitudes (taken as constant) have been fitted in the range $T_c^* \leq 80$ MeV and $0.2 < W < 0.9$ by NA48/2 [7]. For the electric amplitude, using their parametrization, we obtain at $\mathcal{O}(p^4)$:

$$X_E = \frac{-\operatorname{Re}(E_{DE}/eA_{IB})}{m_K^3\cos(\delta_1^1 - \delta_0^2)} = \frac{3G_8/G_{27}}{40\pi^2 F_\pi^2 m_K^2}\left[E^l(W^2, T_c^*) - \frac{m_K^2 \operatorname{Re}\bar{N}}{m_K^2 - m_\pi^2}\right] \equiv X_E^l - X_E^{CT} , \quad (3)$$

where δ_1^1 (δ_0^2) is the strong phase of E_{DE} (A_{IB}). The E^l represents O_8 and O_{27} induced loop contributions (loop contributions from O_{ew} are sub-leading) and $\bar{N}$ corresponds to local counterterms and Q_γ^- contributions. Naively we would expect the O_{27} contributions to be sub-dominant, however, they are dynamically enhanced by $\pi\pi$ loops. Since experimentally, no slope were included in X_E, we average E^l over the experimental range and find $X_E^l = -17.6$ GeV^{-4}. Knowing X_E^l and using the experimental measurement of $X_E = (-24 \pm 4 \pm 4)$ GeV^{-4} we can extract the local contributions

$$X_E^{CT}/X_E^l = 0.37 \pm 0.32 \quad \to \quad \operatorname{Re}\bar{N} = 0.095 \pm 0.083 . \quad (4)$$

To our knowledge it is the first time that $K^+ \to \pi^+\pi^0\gamma$ counterterms contributions are extracted from experiment. The value we found is much smaller than the $\mathcal{O}(1)$ expected for the N_i on dimensional grounds or from factorization [8]. Note that the required amount of counterterm contribution would have been bigger if O_{27} loops were neglected since then $X_E^l = -10.2$ GeV^{-4}. This result is important since it implies that the counterterms combination $\bar{N}$, which appears in other radiative K decays, is now under control and further reliable theoretical investigations can be carried on, in particular concerning the CP violating observables.

3.2 Direct CP-violating asymmetry

Since the bremsstrahlung and direct emission amplitudes interfere and carry different strong and weak phases, a non vanishing CP violating asymmetry can be generated. The asymmetry measures direct CP violation since $K^\pm$ do not mix. Besides and because the long-distance bremsstrahlung amplitude dominates the branching, this CP asymmetry is the simplest window on short-distance physics and a fortiori on possible NP effects. CP-violation in $K^+ \to \pi^+\pi^0\gamma$ is quantified by the parameter $\varepsilon'_{+0\gamma}$, defined from

$$\mathrm{Re}\left(\frac{E_{DE}}{eA_{IB}}\right)\left(K^\pm \to \pi^\pm\pi^0\gamma\right) \approx \frac{\mathrm{Re}\,E_{DE}}{e\,\mathrm{Re}\,A_{IB}}\left[\cos(\delta_1^1-\delta_0^2) \mp \sin(\delta_1^1-\delta_0^2)\varepsilon'_{+0\gamma}\right] , \tag{5}$$

as $\varepsilon'_{+0\gamma} \equiv \mathrm{Arg}E_{DE} - \mathrm{Arg}A_{IB}$ (see [9]). Both Q_γ^- and Q_i (through loops and counterterms) contribute to this parameter and we find

$$\varepsilon'_{+0\gamma}(Q_i) = -0.55(25)\frac{\sqrt{2}|\varepsilon'_K|}{\omega} \quad \text{and} \quad \varepsilon'_{+0\gamma}(Q_\gamma^-) = +2.8(7)\frac{\mathrm{Im}\,C_\gamma^-}{G_F m_K} , \tag{6}$$

respectively[b]. Sadly, these contributions interfere destructively implying that $\varepsilon'_{+0\gamma}|_{\mathrm{SM}} = 0.5(5)\times 10^{-4}$. This large uncertainty is driven by a large uncertainty on counterterms and on estimated $\mathcal{O}(p^6)$ effects. However, contrary to what happens in ε'_K, $\varepsilon'_{+0\gamma}$ is rather insensitive to isospin breaking effects, conservatively taken into account in (6). Expressing $\varepsilon'_{+0\gamma}(Q_i)$ in term of the experimental ε'_K allows us to keep possible NP effects in Q_i under control. As a consequence, the only way for NP to affect $\varepsilon'_{+0\gamma}$ is via its $\mathrm{Im}\,C_\gamma^-$ component. The current bound obtained by NA48/2 [7] is rather weak and allows very large NP effects in $\varepsilon'_{+0\gamma}$:

$$\mathrm{Im}\,C_\gamma^-|_{NP}/G_F m_K = -0.08 \pm 0.13 . \tag{7}$$

4 $K^+ \to \pi^+\pi^0\gamma$ beyond the SM

Once combined with other short-distance sensitive observables, any experimental improved measurement of $\varepsilon'_{+0\gamma}$ will be greatly rewarding. The main problem when probing NP is the issue of disentangling correlations between various NP sources in a fully model-independent way. In [10], we analysed broad classes of NP scenarios defined as model-independently as possible and identified corresponding strategies to constrain and disentangle NP sources using experimental informations on $K_L \to \pi\ell^+\ell^-$, $K \to \pi\nu\bar{\nu}$ decays and $\mathrm{Re}(\varepsilon'_K/\varepsilon_K)$. Doing so we highlighted the complementary informations that could be obtained from radiative decays.

In the MSSM [11–16], NP can affect all the operators in (1) as well as gluon-penguin (denoted by $Q_g^\pm$) and semi-leptonic operators, in particular $Q_{V,l} = \bar{s}\gamma_\mu d \otimes \bar{\ell}\gamma^\mu\ell$. In this particular model the irreducible correlations are two fold. First Q_γ^+ and $Q_{V,l}$ ($\ni Q_{\gamma^*}^+$) always interfere in $K_L \to \pi\ell^+\ell^-$ in and beyond the SM and second, $\mathrm{Re}(\varepsilon'_K/\varepsilon_K)$ receives NP contributions from many different sources. The corresponding bounds are displayed in Figure 1 where we see that a large but not impossible cancellation between NP in gluon-penguin and electroweak operators in $\mathrm{Re}(\varepsilon'_K/\varepsilon_K)$ allows for $\mathrm{Im}C_\gamma^+$ to reach the percent level if we impose $\mathrm{Im}\,C_\gamma^+ = \pm 1.5\,\mathrm{Im}\,C_g^-$. This value will correspond to a saturation of the current $K_L \to \pi^0 e^+e^-$ upper bound and since in the MSSM $Q_\gamma^\pm$ and $Q_g^\pm$ mix under renormalization this $\mathrm{Im}C_\gamma^+$ upper bound provides also an lower bound for $\mathrm{Im}C_\gamma^-$. From (6) this implies that NP can push $\varepsilon'_{+0\gamma}$ up to roughly two orders of magnitude above its SM prediction. The parameter $\varepsilon'_{+0\gamma}$ provides therefore a very good probe for NP γ-penguin effects and furthermore reveals NP cancellations occurring inside $\mathrm{Re}(\varepsilon'_K/\varepsilon_K)$.

[b] Numerically, in the SM, the Wilson coefficient of the magnetic operator in $b \to s\gamma$ can be used for $\mathrm{Im}\,C_\gamma^\pm$, since the CKM elements for the u, c, and t contributions scale similarly and we find $\mathrm{Im}\,C_\gamma^\pm(2\text{ GeV})_{\mathrm{SM}}/G_F m_K = \mp 0.31(8) \times \mathrm{Im}\,\lambda_t$.

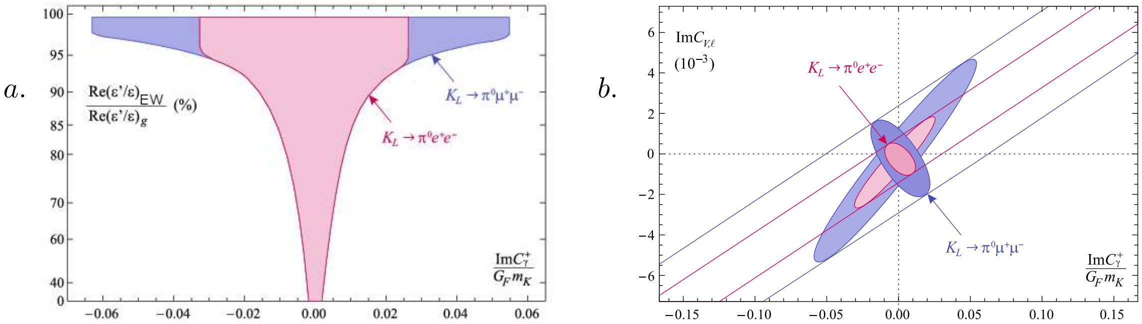

Figure 1: Loop-level FCNC scenario, with all the electroweak operators as well as $Q^{\pm}_{\gamma,g}$ simultaneously turned on, but imposing $\mathrm{Im}\, C^{+}_{\gamma} = \pm 1.5\, \mathrm{Im}\, C^{-}_{g}$ and $|\,\mathrm{Re}(\varepsilon'_K/\varepsilon_K)^{\mathrm{NP}}| < 2\,\mathrm{Re}(\varepsilon'_K/\varepsilon_K)^{\mathrm{exp}}$. (a) The $\mathrm{Im}\, C^{+}_{\gamma}$ range as a function of the fine-tuning between $\mathrm{Re}(\varepsilon'_K/\varepsilon_K)_{EW}$ and $\mathrm{Re}(\varepsilon'/\varepsilon)_g$. (c) The corresponding contours in the $\mathrm{Im}\, C_{V,\ell} - \mathrm{Im}\, C^{+}_{\gamma}$ plane. In (b), the lighter (darker) colors denote destructive (constructive) interference between NP γ^*-penguin and Q^{+}_{γ} in $K_L \to \pi^0 \ell^+ \ell^-$.

5 Conclusion

We exemplify in $K^+ \to \pi^+ \pi^0 \gamma$ that the stage is now set theoretically to fully exploit the $s \to d\gamma$ transition. The SM predictions are under good control, the sensitivity to NP is excellent, and signals in rare and radiative K decays not far from the current experimental sensitivity are possible. Thus, with the advent of the next generation of K physics experiments (NA62 at CERN, K0TO at J-Parc, ORKA at Fermilab and KLOE-II at the LNF), the complete set of flavor changing electromagnetic processes, $s \to d\gamma$, $b \to (s,d)\gamma$, and $\ell \to \ell' \gamma$, could become one of our main windows into the flavor sector of the NP which will hopefully show up at the LHC.

Acknowledgments

I thank the organizers of the *Rencontres de Moriond EW 2012* for the pleasant and stimulating stay and for their financial support. I warmly thank Christopher Smith for the fruitful collaboration at the origin of this work. I'm also grateful to him and Jean-Marc Gérard for their valuable suggestions and comments about the present note.

References

1. G. Colangelo, G. Isidori and J. Portoles, Phys. Lett. B **470** (1999) 134.
2. G. Buchalla, A. J. Buras and M. E. Lautenbacher, Rev. Mod. Phys. **68** (1996) 1125.
3. F. E. Low, Phys. Rev. **110** (1958) 974.
4. J. Kambor, J. H. Missimer and D. Wyler, Nucl. Phys. B **346** (1990) 17.
5. G. Ecker, J. Kambor and D. Wyler, Nucl. Phys. B **394** (1993) 101.
6. N. Christ, Phys. Rev. **159** (1967) 1292.
7. J. R. Batley *et al.* [NA48/2 Collaboration], Eur. Phys. J. C **68** (2010) 75.
8. G. Ecker, H. Neufeld and A. Pich, Nucl. Phys. B **413** (1994) 321.
9. G. D'Ambrosio and G. Isidori, Int. J. Mod. Phys. A **13** (1998) 1.
10. P. Mertens and C. Smith, JHEP **1108** (2011) 069.
11. A. J. Buras and L. Silvestrini, Nucl. Phys. B **546** (1999) 299.
12. A. J. Buras et al. , Nucl. Phys. B **566** (2000) 3.
13. F. Mescia, C. Smith and S. Trine, JHEP **0608** (2006) 088.
14. G. Colangelo and G. Isidori, JHEP **9809** (1998) 009.
15. G. Isidori, F. Mescia, P. Paradisi, C. Smith and S. Trine, JHEP **0608** (2006) 064.
16. A. J. Buras, T. Ewerth, S. Jager and J. Rosiek, Nucl. Phys. B **714** (2005) 103.